ADVANCED FUNCTIONAL MATERIALS
www.afm-journal.de

Graphene-Directed Supramolecular Assembly of Multifunctional Polymer Hydrogel Membranes

*Yufei Wang, Sheng Chen, Ling Qiu, Kun Wang, Huanting Wang, George P. Simon, and Dan Li**

Polymer-based nanoporous hydrogel membranes hold great potential for a range of applications including molecular filtration/separation, controlled drug release, and as sensors and actuators. However, to be of practical utility, polymer membranes generally need to be fabricated as ultrathin yet mechanically robust, have a large-area yet be defect-free and in some cases, their structure needs the capability to adapt to certain stimuli. These stringent and sometimes self-conflicting requirements make it very challenging to manufacture such bulk nanostructures in a controllable, scalable and cost-effective manner. Here, a versatile approach to the fabrication of multifunctional polymer-based hydrogel membranes is demonstrated by a single step involving filtration of an aqueous dispersion containing chemically converted graphene (CCG) and a polymer. With CCG uniquely serving as a membrane- and pore-forming directing agent and as a physical cross-linker, a range of water soluble polymers can be readily processed into nanoporous hydrogel membranes through supramolecular interactions. With the interconnected CCG network as a robust and porous scaffold, the membrane nanostructure can easily be fine-tuned to suit different applications simply by controlling the chemistry and concentration of the incorporated polymer. This work provides a simple and versatile platform for the design and fabrication of new adaptive supramolecular membranes for a variety of applications.

1. Introduction

Molecule- and ion-permeable synthetic polymer membranes are key components in many important industrial processes such as water purification and desalination, the concentration and fractionation of mixtures in the food and drug industries and in energy storage and conversion devices.[1] Compared to other separation-related technologies such as distillation, membrane separation is a low-cost, energy efficient and green technology.[2] In these and other applications, it is increasingly desirable that the membranes can be made "smart" in that they are able to respond to external stimuli such as temperature, pH, salt concentration or certain chemicals, effectively mimicking the hydrogel membranes in living systems such as skin.[3] Such smart synthetic membranes hold great promise for application in a number of biomedical areas such as artificial organs, drug delivery systems, chemical or biological sensors and diagnostic devices.[4]

The great potential of polymer membranes for these emerging applications, particularly those based on stimuli-responsive hydrogels, has resulted in extensive research efforts in membrane synthesis. A number of techniques such as layer-by-layer assembly, surface grafting, block-copolymer self-assembly and templating have been recently developed.[3c,5] Although polymer hydrogel membranes prepared by these methods can display certain functionalities, their eventual utilization in a commercial scenario still requires a series of issues to be properly addressed and resolved, such as mechanical and chemical stability and the degree of perfection of the membrane. The mechanical stability is not just of the membrane in the macroscopic scale, but also relates to the ability of the incorporated, active polymer component to be retained in the membrane. This is particularly difficult for hydrogel films which are intrinsically weak, and for smart membranes where repetitive stimuli-induced configuration transition of polymer may lead to mechanical degradation of the membrane.[3a] Whilst maintaining mechanical stability, it is also highly desired to make the membranes very thin as this enables a fast response and high flux. Making such thin membranes over a large area is also very desirable, but the possibility of flaws increases. Importantly, the membrane materials must themselves not impede the external stimuli, and be readily able to be surface-modified to tailor the behavior of the membrane. Increasingly, multiple functionalities are being sought in such membranes.[3a-c] One such desired functionality is electrical responsiveness, yet most smart polymer membranes reported in the literature[3a-c,5] are not electrically conductive and their permeation cannot be regulated by electrical potential unless the membranes

Y. Wang, Dr. S. Chen, L. Qiu, Prof. G. P. Simon, Prof. D. Li
Department of Materials Engineering
Monash University
VIC 3800, Australia
E-mail: dan.li2@monash.edu
Dr. K. Wang and Prof. H. Wang
Department of Chemical Engineering
Monash University
VIC 3800, Australia

DOI: 10.1002/adfm.201402952

are grown on electrically conductive substrates or electrically conductive nano-fillers are used. The need to meet all these requirements and to properly engineer the membrane structure at multiple length scales (from molecular-, micro-, nano- to macroscopic) poses a great challenge to fabrication of such functional polymer membranes in a controllable, scalable and cost-effective manner.

This work reports that the use of chemically converted graphene (CCG) to direct the interfacial gelation of water soluble polymers can provide a very efficient approach to address this challenge. Graphene can be considered as a very large macromolecule with a unique two-dimensional (2D) molecular configuration.[6] Recent research has shown that chemically modified graphene sheets such as graphene oxide and reduced graphene oxide (or CCG) are able to self-assemble in a face-to-face manner under filtration, readily forming uniform, mechanically stable and liquid/gas permeable membranes with peculiar molecular and ionic transport behaviors.[7] In this work, we demonstrate a new, versatile application of graphene for membrane technology: the use of CCG to guide ordinary water-soluble polymers to form ultrathin, robust supramolecular hydrogel membranes through a facile filtration process. In particular, we show that CCG can function more than just highly effective nanofiller for mechanical and electrical reinforcement in polymer composites, as is widely reported in the literature.[8] Rather, its micro-corrugated molecular configuration, unique self-assembly behavior and rich supramolecular interactions with traditional polymers allow it to act as an unprecedented membrane- and pore-forming directing agent and a physical cross-linker for traditional polymers. The judicious utilization of such multiple roles of CCG sheets thus represents a new concept for the efficient design and fabrication of functional polymer membranes.

2. Results and Discussion

2.1. Formation of Robust and Porous Polymer/CCG Hydrogel Membranes

Poly(*N*-isopropylacrylamide) (PNIPAM), a widely studied stimuli-responsive polymer, was selected to demonstrate our concept. PNIPAM is known to undergo reversible globule-to-coil configuration transition at its lower critical solution temperature (LCST), and its stimuli-responsive behavior has long been utilized for fabrication of smart membranes.[9] In this work, aqueous dispersions containing PNIPAM and CCG with a range of mass ratios of PNIPAM to CCG ($R_{P/C}$) are readily prepared by simply mixing aqueous PNIPAM solution and CCG dispersion. A series of PNIPAM/CCG membranes with different $R_{P/C}$ can be obtained by filtration of the mixed dispersions (**Figure 1**a). As with the filtration of CCG alone,[10] pressure-driven filtration of the mixture leads to the formation of a black film on the filter membrane, and its thickness gradually increases during the filtration process. The remaining dispersion on top of the membrane maintains an unchanged CCG concentration without aggregation (Figure S1, Supporting Information). The membrane formation process is complete when the free solution drains through the formed membrane, with the black film (if sufficiently thick) able to be peeled off from the supporting filter (Figure 1b). The resultant PNIPAM/CCG membranes contain over 82 wt% of water, indicative of their hydrogel nature.

Interestingly, nearly all of the PNIPAM molecules are retained in the hydrogel film with $R_{P/C}$ up to 3. This can be confirmed by both the total weight measurement of the dried films (Figure S2, Supporting Information) and thermogravimetric analysis (TGA) (Figure S3a), showing little PNIPAM (< 1wt%) escaped from the filter during filtration, even in the

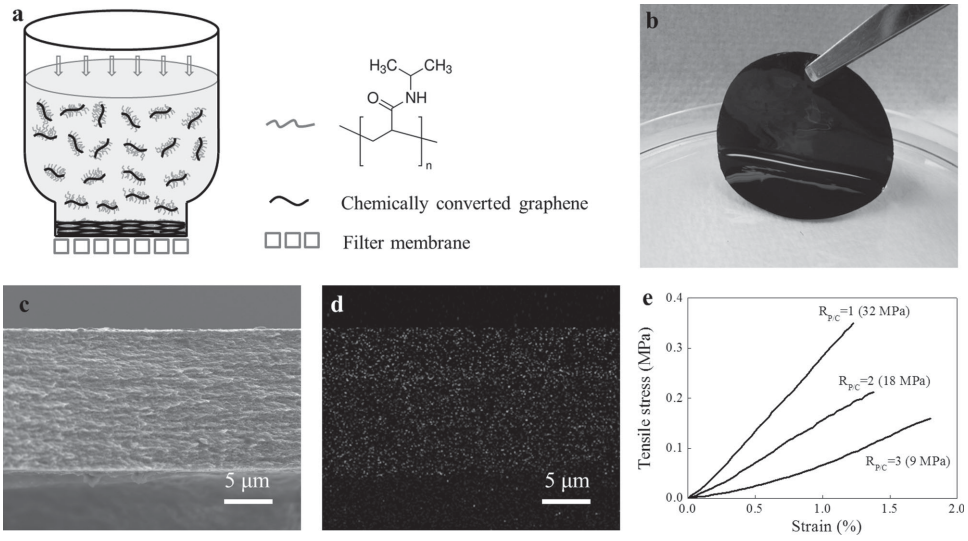

Figure 1. Formation of robust and porous PNIPAM/CCG hydrogel membrane. a) Schematic diagram of the formation of PNIPAM/CCG hydrogel membrane by pressure-driven filtration; b) Photograph of an as-formed PNIPAM/CCG hydrogel membrane ($R_{P/C} = 2$) (prepared by 4.5 mg of CCG and 9 mg of PNIPAM); c) SEM image and d) EDX mapping of the element N of the cross-section of dried PNIPAM/CCG membrane ($R_{P/C} = 2$); e) Strain-stress curves of PNIPAM/CCG hydrogel membranes with different mass ratio of PNIPAM to CCG ($R_{P/C}$).

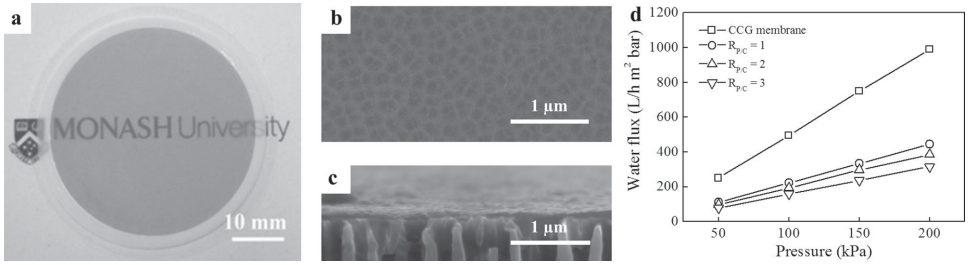

Figure 2. Characterization of ultrathin PNIPAM/CCG hydrogel membranes. a) A photograph of an ultrathin PNIPAM/CCG hydrogel membrane ($R_{P/C}$ = 2) on an anodic aluminium oxide filter membrane, and SEM images of its b) top view and c) cross-sectional view; d) Water flux of ultrathin CCG and PNIPAM/CCG hydrogel membranes with different $R_{P/C}$ as a function of pressure.

case of high content of PNIPAM ($R_{P/C}$ = 3). Scanning electron microscopy (SEM) images of the cross-section of the dried PNIPAM/CCG membranes show a uniform structure without obvious aggregates (Figure 1c and Supporting Information Figure S4a,b). Moreover, both SEM images and energy-dispersive X-ray (EDX) elemental mapping of nitrogen (Figure 1d and Supporting Information Figure S4c,d) reveal a uniform distribution of PNIPAM throughout the film. The presence of PNIPAM in the hybrid hydrogel film is also confirmed by Fourier-Transform Infrared Spectroscopy (FTIR) (Figure S3b, Supporting Information). The above results indicate that both PNIPAM and CCG have been uniformly and continuously co-deposited on the filter during filtration, leading to the formation of a hybrid hydrogel membrane.

The tensile test of these hybrid membranes reveals a Young's modulus of 9–32 MPa for the as-formed PNIPAM/CCG hydrogel membranes with $R_{P/C}$ up to 3 (Figure 1e). These values are several orders of magnitude higher than that of conventional synthetic polymer hydrogels with the similar water content (which lie in the kPa range).[11] Furthermore, the mechanical integrity of all the PNIPAM/CCG hydrogel films with $R_{P/C}$ up to 3 can be retained in water for at least 1 month (Figure S5a, Supporting Information) and little leakage of polymer from the membrane is observed.

The mechanical integrity of the hybrid hydrogel films is further demonstrated by the ease with which the large-area, ultrathin PNIPAM/CCG hydrogel membranes can be formed using the same procedure but with a very small amount of material. **Figure 2**a shows an image of a PNIPAM/CCG hydrogel membrane with ≈3.5 cm in diameter which contains only 36 μg of PNIPAM and 18 μg of CCG (≈24 layers of CCG, see Supplementary Methods). The SEM images of its dried state shows a rather smooth and uniform surface with a thickness of about 20 nm (Figure 2b,c). Importantly, although the membrane is very thin, almost all of the PNIPAM molecules are retained in the membrane. This was confirmed by UV–Vis characterization and total organic carbon (TOC) analysis of the filtrate solutions collected during the membrane formation (see Methods, Figure S6, and Table S1 in the Supporting Information). Moreover, the uniform, ultrathin PNIPAM/CCG hydrogel membranes yield high water permeability (**Figure 3**b,d and Supporting Information Figure S7) which is comparable to that of carbon-based nanofiltration membranes.[12] The permeation results also suggest that the membranes are stable for at least

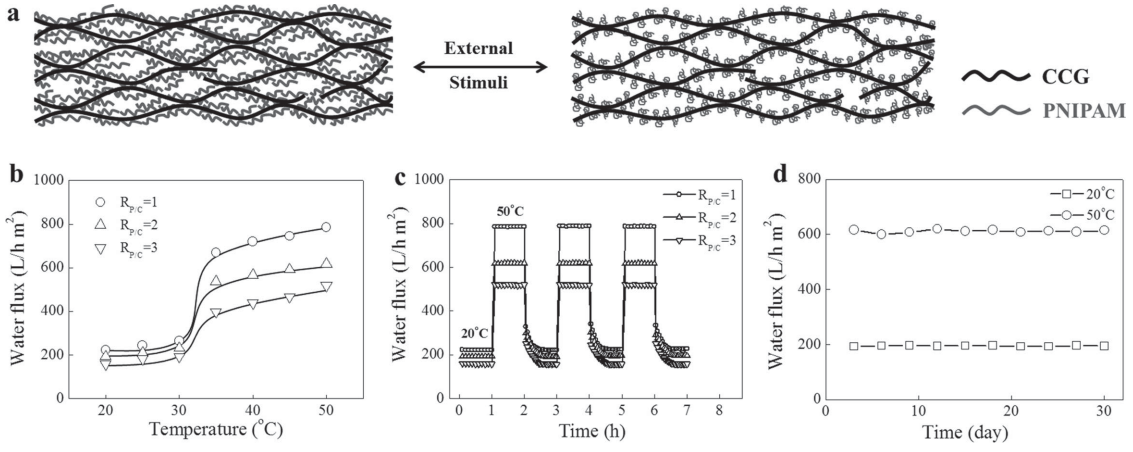

Figure 3. Microstructure and water permeation performance of PNIPAM/CCG hydrogel membranes. a) Schematic diagram of the proposed structure of PNIPAM/CCG hydrogel membrane, showing stimuli-responsive tuning of its porous structure; b) water flux of ultrathin PNIPAM/CCG hydrogel membranes with different mass ratios as a function of temperature at 100 kPa and c) their excellent reversibility between 20 °C and 50 °C; d) Long term stability of an ultrathin PNIPAM/CCG hydrogel membrane ($R_{P/C}$ = 2) at 20 °C and 50 °C, respectively.

one month (Figure 3d) and can sustain pressures of at least up to 200 kPa (Figure 2d).

2.2. Insights into the Microstructure of Polymer/CCG Hydrogel Membranes

Unlike dried membranes with well-defined pore structures, the as-prepared hydrogel membranes contain liquid and have a dynamic structure, making it very difficult to use traditional microscopic techniques to visualize in situ how the polymer and CCG are distributed at the molecular level. Despite the difficulty of direct micro-characterization, we have developed a number of indirect techniques to probe the microstructure of the polymer/CCG hydrogel membranes. Here, we made use of the well-known configuration transition behavior of PNIPAM and by carrying out water permeation experiments to shed light on the dynamic structure of the hydrogel membranes. The ability to manipulate PNIPAM in this way is one of the reasons why it was chosen as our model polymer.

All of the thin membranes are found to be stable and highly permeable to water, indicative of a porous structure in the membrane. The thickness of PNIPAM/CCG hydrogel membranes is very close to that of polymer-free CCG hydrogel membrane (Table S2, Supporting Information), and is nearly independent of the amount of polymer or temperature. This suggests that the PNIPAM molecules are trapped in between the CCG sheets, which is consistent with the observation that the water flux of PNIPAM/CCG membrane decreases with the polymer content in the membrane (Figure 3b). Moreover, for all the PNIPAM/CCG hydrogel membranes, the water flux gradually increases with temperature, and presents a sharp increase when the temperature is increased between 30 °C and 35 °C, within the LCST of PNIPAM (Figure 3b).[9a] Such a sudden change of water flux is not observed in the CCG-only hydrogel membrane where the water flux increases almost linearly with temperature as a result of the viscosity change of water (Figure S8, Supporting Information).[13] This result indicates that the PNIPAM in the membrane has conferred its temperature-responsive behavior to the hybrid hydrogel membrane.

On the basis of the above observations, we propose the microstructure of PNIPAM/CCG hybrid hydrogel membranes as is shown in Figure 3a. We have previously found that CCG sheets dispersed in water have a micro-corrugated molecular configuration.[14] Vacuum filtration of CCG dispersion results in the formation of an oriented hydrogel film in which CCG sheets are physically cross-linked through van der Waals attractions and hydrophobic forces but exhibit a much larger interlayer distance (≈12 nm) than graphite (0.34 nm) as a result of being micro-corrugated and due to intersheet hydration and electrostatic repulsions.[10] As with polymer-free CCG hydrogels, the micro-corrugated CCG sheets in the hybrid hydrogel films are physically linked together to form a continuous and highly porous network, which can be confirmed by the high electrical conductivity of the membranes ($R_{P/C} \leq 3$, Supporting Information Table S2). We speculate that the polymer molecules are adsorbed on and trapped between the CCG sheets through van der Waals attractions and other intermolecular forces such as hydrogen bonding and hydrophobic forces. As a result of such a polymer inclusion, the pore size of the membranes becomes smaller and the pore surface chemistry is modified, making it possible to use the membrane for molecular separation (see examples in the following section). It is worth noting that despite the slit-like pores normally presenting a tortuous path to a permeate such as water, membranes with a reasonably high flux can still be made because of the ability to make them ultrathin (Figure 2b). Additionally, the stimuli-responsiveness of PNIPAM molecules is well maintained in the membranes. Manipulation of the stimuli-responsive behavior of PNIPAM allows this to be transmitted to the PNIPAM/CCG ensemble, enabling reversible stimuli-induced regulation of pore size and hence permeability of water (Figure 3b,c).

2.3. Versatility of Polymer/CCG Hydrogel Membrane Formation

We have also tested many other water soluble polymers for inclusion, including temperature and pH sensitive poly(*N*-isopropylacrylamide-co-acrylic acid) (PNIPAM-AA), temperature and glucose sensitive poly(*N*-isopropylacrylamide-co-phenylboronic acid) (PNIPAM-PBA), poly(ethylene-oxide) (PEO), poly(vinyl alcohol) (PVA) and biomolecules such as DNA. A stable aqueous dispersion containing the selected polymer and CCG is achievable simply by mixing the two aqueous solutions, and filtration of the mixed aqueous dispersion ($R_{P/C} \leq 3$) leads to the formation of various robust and porous polymer/CCG hybrid hydrogel membranes. Unlike conventional polymer hydrogels,[3b] the formation of polymer/CCG hydrogel membranes is achieved in a single filtration step and no specifically designed chemical bonding nor stringent processing conditions are required. It appears that so long as the affinity of the polymer to CCG is sufficiently strong, the polymer can be readily processed into a hydrogel membrane using this simple approach (Figure S9, Supporting Information).

2.4. Unique Roles of CCG in Membrane Formation and Potential Implications

The crucial roles that CCG sheets play in the formation of these polymer hydrogel membranes are discussed below to further illustrate the underpinning mechanism and potential implications of the CCG-directed membrane design and fabrication concept.

Firstly, CCG sheets act as a molecular carrier or directing agent for membrane formation to allow the co-deposition of CCG and the adsorbed polymer molecules on the filter membrane during the filtration process, greatly simplifying the membrane fabrication process. Although there is no strong chemical bond between the polymer and CCG sheets, the giant molecular size of CCG as well as residual oxygen-containing groups appear able to lead to a strong collective non-covalent supramolecular interactions between CCG and the polymer molecules (see Supplementary Methods and Figure S10 in the Supporting Information). These interactions can then enable co-deposition of CCG and polymer molecules during filtration and eventually constrain them between CCG sheets in the

resultant membrane. This must occur because otherwise the water soluble polymer molecules would simply flow through the filter and not be trapped in the membrane (unless they are chemically cross-linked on the filter as previously reported[15].

Secondly, the CCG sheets are an integral part of the hybrid hydrogel membranes to maintain their structural and mechanical integrity. For most of the hydrogel membranes produced and tested in this work, the polymer is the majority phase, and CCG sheets can serve as a reinforcing nanofiller or a cross-linker to strengthen the membrane as those in traditional graphene/polymer composites. Moreover, the CCG sheets can assembly into a continuous network embedded in the polymer matrix (see proposed membrane structure in Figure 3a) which physically links the polymer molecules together to form a robust structure. The face-to-face stacking manner of CCG sheets particularly favors the linkage between CCG and polymer because the polymer molecules have the possibility to interact with both adjacent CCG sheets, linking them together. This can be evidenced from the slight thickness reduction of PNIPAM/CCG hydrogel membranes compared to that of CCG membrane (Table S2, Supporting Information). Differing from previously reported graphene/polymer hydrogel composites, the collective, mutual supramolecular interactions between CCG and polymer ensure the mechanical integrity of the polymer/CCG hydrogel membranes and account for their long term stability when water passes through them (Figure 3d).

In comparison, tailoring the polymer-CCG interactions may make it unable to trap the polymer molecules tightly in the membrane, resulting in membrane redissolving in water. For example, we have found that when $R_{P/C}$ is above 3, the interconnectivity of CCG network is weakened, and both CCG and PNIPAM molecules cannot link together tightly to maintain structural integrity (Figure S5b, Supporting Information). On the other hand, increasing the amount of polar groups in CCG—replacing CCG by unreduced graphene oxide (GO)—leads to increased repulsive force between GO sheets, making them unable to form a mechanically stable network to accommodate polymers within the membrane (Figure S5c, Supporting Information). As a result, although the non-covalent interaction between GO sheets and polymer is enhanced, the lack of a mechanically stable scaffold in the polymer hydrogel membrane results in membrane redissolving in water.

Thirdly, the use of CCG makes it possible to tune the membrane structure in a much simplified and versatile manner compared with other systems. Practically useful membranes require careful engineering of their structure at all levels from molecular, nano- to macroscopic scales. In our design, the interconnected continuous CCG network not only provides a robust scaffold for polymers to ensure a reasonably high macroscopic mechanical strength and structural uniformity, but also pre-defines the nanostructure of the membrane through its self-assembled nanoporous structure. Fine-tuning of the pore structure and chemistry of the membranes can be readily realized by the incorporation of selected polymers during the filtration process. In contrast, the traditional membrane fabrication techniques such as spin-coating generally require optimising all of the processing conditions such as type of solvent used, temperature, atmosphere, and pre- or post-treatments. When a new polymer or application is targeted, it is often necessary to change the entire fabrication procedure, which generally requires substantial experimental trials and is very time-consuming and expensive.

The exceptional simplicity and versatility of the CCG-directed membrane formation approach greatly facilitates the design and fabrication of a range of functional membranes to suit various applications. For example, it has been reported that the molecular configuration of PNIPAM modified with acrylic acid groups (PNIPAM-AA) and phenylboronic acid (PNIPAM-PBA) is sensitive to pH[3b] and glucose,[16] respectively. We have found that both PNIPAM-AA and PNIPAM-PBA can be incorporated into the fabricated hybrid hydrogel membranes using the same procedure. The resultant hydrogel membranes are indeed found to be responsive to pH (**Figure 4**a) and glucose (Figure 4b), respectively.

Furthermore, the simplicity of this membrane formation approach makes it a particularly attractive methodology to rapidly screen new polymers for membrane applications. For example, our preliminary experiments have revealed that the PNIPAM/CCG membrane displays very different separation behavior for Rhodamine B (Figure 4c) and Copper(II) phthalocyanine-tetrasulfonic acid tetrasodium salt (Figure 4d) and DNA/CCG hybrid hydrogel membranes prepared using this approach can effectively reject ferritin (a commonly used protein) (Figure S11). Unfortunately, we do not fully understand the separation mechanism at the stage because that molecular separation is essentially a very complex process which can be influenced by many factors, such as pore size, pore wall chemistry and pore density. However, our prelimiary results suggest that the polymer/CCG hydrogel membranes can serve as a readily available experimental platform to study how certain molecules interact with the polymers, which will provide much-needed information for future membrane design.

Additionally, the electrically conductive and strongly light-absorbing CCG network has the potential to offer extra electrical and optical functionalities to the polymer/CCG hydrogel membranes. Our initial experiments show that the flux of water through polymer/CCG hydrogel membrane changes with the application of electric field (Figure 4e). This is likely due to the change in the dissociation degree of carboxylic groups in CCG under electrical stimulation, which results in varied interlayer spacing between CCG sheets. Additionally, since graphene has a high light absorption capacity, we have also observed local heating effect of PNIAPM/CCG hydrogel membranes caused by photo-thermal effect of graphene upon exposure to a light stimulus. This results in the shift of the water flux transition temperature from ≈32 °C to ≈28 °C (Figure 4f), indicating the volume transition of PNIPAM at an external temperature lower than its LCST under light stimulus.

It is worth noting that the polymer/CCG membrane structure makes it very easy to realize structurally adaptive yet mechanically robust "smart" membranes. Such features are usually very challenging for most traditional synthetic hydrogel membranes to achieve as they usually suffer from mechanical weakness. The use of cross-linkers (i.e., covalent approach) to alleviate this problem, however, may significantly limit the chain mobility and restrict the stimuli-responsive behavior of polymer molecules, making structural adaptivity of the membrane contradictory to its mechanical robustness.[3b,c]

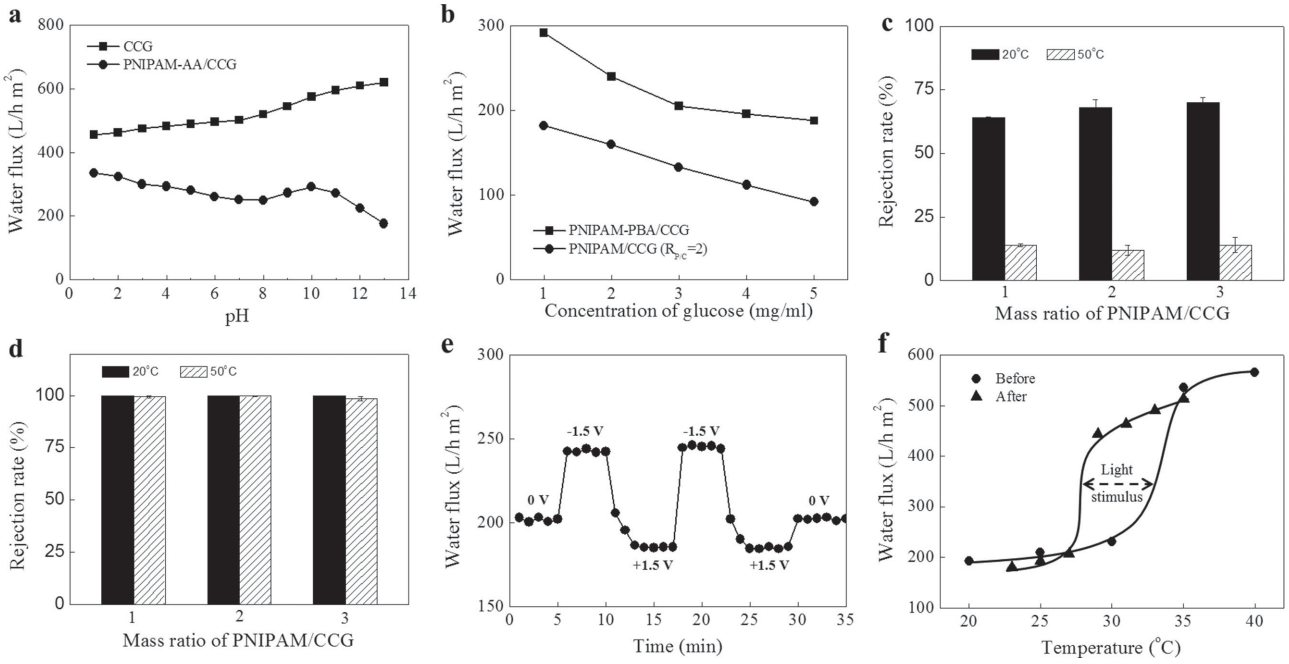

Figure 4. CCG-directed supramolecular membrane assembly as a simple and versatile approach to multi-functional polymer hydrogel membranes. a) Water flux of ultrathin CCG and PNIPAM-AA/CCG hydrogel membranes as a function of pH at 25 °C; The increased water flux of CCG membrane with raising pH is due to increased degree of ionization of carboxylic groups on CCG sheets, leading to increased inter-sheet repulsion and consequently larger nanochannel size. The increase in pH value, in general, also leads to swelling of AA molecules. Thus, the configuration change of AA and interlayer spacing changeof CCG sheets together contribute to water flux change of PNIPAM-AA/CCG. b) Water flux of ultrathin PNIPAM-PBA/CCG and PNIPAM/CCG ($R_{P/C}$ = 2) hydrogel membranes as a function of glucose concentration. The PBA molecules can interact with glucose to form a stable complex with volume shrinkage in weak alkaline environment, and this is likely the reason for glucose responsive change of water flux of PNIPAM-PBA/CCG hydrogel membrane. Rejection rate of c) Rhodamine B and d) Copper(II) phthalocyanine-tetrasulfonic acid tetrasodium salt from ultrathin PNIPAM/CCG hydrogel membranes with different $R_{P/C}$ at 20 °C and 50 °C, respectively; Water flux of an ultrathin PNIPAM/CCG hydrogel membrane ($R_{P/C}$ = 2) in response to e) electric field and f) light stimulus. Note that for light stimulus experiment, the temperature of water just above the membrane was measured, and water flux of the membrane before and after applying a light source (radiation intensity: 700 W/m^2) as a function of temperature was recorded. All the filtration experiments were conducted on an anodic aluminium oxide filter membrane at 100 kPa.

Such example have been demonstrated by highly cross-linked PNIPAM copolymer multilayers which exhibit very limited swelling ratio.[3c,17] Using multiple strong non-covalent interactions to assemble stimuli-responsive polymers represents a promising approach to realizing adaptive materials.[18] In our membrane design, because the mechanical strength is mainly contributed by the supramolecular interaction between polymer molecules and CCG network and the incorporated polymer is not chemically cross-linked, the stimuli-responsive properties of the polymer can largely be retained and readily transferred to the hybrid membrane while maintaining mechanical robustness. This concept may greatly facilitate the development of emerging biomimetic, adaptive supramolecular materials.[18a,b]

3. Conclusion

In conclusion, we have demonstrated that a series of mechanically robust and structurally tuneable polymer/CCG hydrogel membranes can be prepared by simple filtration of the mixture containing CCG and selected polymer. The CCG sheets play multiple key roles as both a membrane- and pore-forming directing agent, as structural reinforcement nanofiller and as a physical cross-linker in the membrane formation process, drastically simplifying the design and fabrication of functional polymer-based hydrogel membranes. The simplicity and versatility of this fabrication approach makes it very promising for the development of adaptive supramolecular materials.

4. Experimental Section

Materials: Poly(*N*-isopropylacrylamide-co-acrylic acid) (PNIPAM-AA) and poly(*N*-isopropylacrylamide-co-phenylboronic acid) (PNIPAM-PBA) were synthesized by the following process. Acrylic acid (AA, 30 mg, Sigma-Aldrich) or phenylboronic acid (PBA, 10 mg, Sigma-Aldrich) was mixed with *N*-isopropylacrylamide (NIPAM) monomers (200 mg, Sigma-Aldrich), ammonium persulfate (APS, 60 mg) and *N,N,N′,N′*-Tetramethylethylenediamine (TEMED, 2 drops) in distilled water (20 mL). The mixtures were then sealed in a glass tube and polymerized for 24 h at room temperature. The excess ions in the mixtures were removed using a dialysis tubing cellulose membrane (molecular weight cut-off: 14 000; Sigma-Aldrich) against deionized water for one week, and the as-obtained PNIPAM-AA and PNIPAM-PBA solutions were diluted to required concentration (1 mg/mL). The glucose solutions with different concentrations used for filtration were prepared by dissolving corresponding amount of α-D-glucose (Sigma-Aldrich) in Na_2CO_3-$NaHCO_3$ buffer solution (0.1 mol/L; pH = 9). Additionally, polyethylene oxide (PEO) and poly(vinyl alcohol) (PVA) with different

molecular weights, Deoxyribnucleic acid (DNA) from herring sperm, Ferritin from horse spleen, rhodamine B and Copper(II) phthalocyanine-tetrasulfonic acid tetrasodium salt were all obtained from Sigma-Aldrich.

Fabrication of Polymer/CCG Hydrogel Membranes: CCG dispersion (0.3 mg/mL) was synthesized by chemical reduction of graphene oxide (GO) colloid using hydrazine as described in our previous work.[19] To fabricate polymer/CCG hydrogel membranes, an aqueous solution containing polymers was initially mixed with CCG dispersion with desired mass ratio of polymer to CCG ($R_{P/C}$). For the preparation of an ultrathin PNIPAM/CCG hydrogel membrane ($R_{P/C}$ = 2), poly(*N*-isopropylacrylamide) (PNIPAM,) solution (36 μL, 1 mg/mL; molecular weight: 19 000–30 000, Sigma-Aldrich) was mixed with CCG dispersion (6 mL, 3 μg/mL). The mixed solution was then diluted by water to a total volume of 20 mL and subject to pressure-driven filtration through a nitrocellulose mixed ester filter membrane (0.2 μm pore size, 47 mm diameter, Sterlitech) using a dead end filtration device (HP4750, Sterlitech). The formation of the hydrogel membrane was completed once the free solution was drained, and distilled water (200 mL) was immediately added to the filtration device, followed by pressure-driven water permeation to stabilize the hydrogel membrane as well as keeping it in hydrated state. All the other polymer/CCG hydrogel membranes were fabricated using the same procedure. The hydrogel membranes were immersed in water for storage.

Estimation of CCG Layers in Ultrathin Polymer/CCG Hydrogel Membranes: Given the area of membrane (9.78 cm^2) and the carbon-carbon distance (0.142 nm) in graphene sheet,[1] the area of each carbon atom in graphene sheet is about 2.61 $Å^2$ and the number of carbon atoms in one CCG layer in the membrane was estimated to be 3.75×10^{16}. The mass of one CCG layer in the membrane is therefore estimated to be $3.75 \times 10^{16} \times 12$ g/mol/$(6.023 \times 10^{23}$/mol) = 0.747 μg. Since 18 μg of CCG was used for membrane assembly, the number of CCG layers was estimated to be 18 μg/0.747 μg = 24 layers.

Optical Characterization of Non-covalent Interactions between CCG and Polymer in Aqueous Solution: The non-covalent interactions between CCG and non-conjugated, water soluble polymers in aqueous solution were characterized by our previously developed method using dye molecules as probes.[20] Typically, the addition of CCG dispersion to 5, 10, 15, 20 – tetrakis (1-methyl-4-pyridinio) porphyrin (TmPyP, Sigma-Aldrich) solution can lead to an adsorption peak shift from 422 nm to 460 nm. The addition of non-conjugated, water soluble polymers, such as polyethylene oxide (PEO) and poly(vinyl alcohol) (PVA), to the TmPyP/CCG mixed system results in the recovery of the absorption peak to 422 nm, indicating strong non-covalent interactions between CCG and PEO or PVA which leads to desorption of π-conjugated molecules from CCG. In addition, the absorbance also changes as a function of the amount of polymer added. We therefore used this method to characterize the non-covalent interaction between CCG and PNIPAM, and also to estimate the amount of polymer which remains uncaptured during the ultrathin membrane formation.

Structural Characterization of Polymer/CCG Hydrogel Membranes: The stress-strain curves were obtained on a dynamic mechanical thermal analyzer (Rheometrics Mark IV DMTA). The hydrogel membrane samples were first cut into 5 mm × 10 mm, and gripped using a film tension clamp. The experiments were conducted in a controlled strain rate mode with the strain ramp rate of 0.01% s^{-1} and a pre-load of 0.02 N. The total dissolved carbon concentration in filtered aqueous solution, which was collected during the formation of polymer/CCG hydrogel membranes, was determined using a Total Organic Carbon Analyzer (TOC-LCSH, Shimadzu) which adopts the 680 °C combustion catalytic oxidation method. The UV–Vis spectra were collected using a Varian Cary 300 UV/Visible spectrometer. The morphology of the membranes was characterized by scanning electron microscope (JEOL JSM 7001F). The FT-IR spectra were recorded on a Nicolet IS-10 spectrometer. Thermogravimetric analysis (Perkin-Elmer SII TG/DTA 6300, Pyris thermogravimetric analyzer) was conducted by thermally scanning from room temperature to 500 °C at a heating rate of 5 °C/min. The electrical conductivity of the membranes was measured by a Jandel four-point probe using a linear array four-point head.

Permeability Characterization of Polymer/CCG Hydrogel Membranes: Both permeation and separation experiments were undertaken using a dead end filtration device (HP4750, Sterlitech). A beaker on the balance was connected to the computer which was used to collect the filtered solution, and water flux was recorded automatically by computer software immediately after membrane formation. Note that the water flux value usually decreased with time in the initial stages, and then stabilized after several hours of the membrane formation (see example in Figure S9, Supporting Information). All of the reported water flux values are derived from the stabilized values. In addition, both a water bath and thermometer were used to control and measure the temperature of the filtration device and the membrane. For electric and light stimulus experiments, a 1.5 V battery and an external light source were connected to the whole device, respectively.

Supporting Information

Supporting Information is available from the Wiley Online Library or from the author.

Acknowledgements

Y.W. and S.C. contributed to this work equally. The authors acknowledge the financial support from the Australian Research Council. This work made use of the facilities at the Monash Center for Electron Microscopy.

Received: August 26, 2014
Revised: September 30, 2014
Published online: October 27, 2014

[1] a) N. Li, A. G. Fane, W. S. W. Ho, T. Matsuura, in *Advanced Membrane Technology and Applications*, John Wiley & Sons, Inc., New Jersey **2008**; b) R. W. Baker, in *Encyclopedia of Polymer Science and Technology*, John Wiley & Sons, Inc., New Jersey **2002**.
[2] T. C. Merkel, B. D. Freeman, R. J. Spontak, Z. He, I. Pinnau, P. Meakin, A. J. Hill, *Science* **2002**, *296*, 519–522.
[3] a) M. A. C. Stuart, W. T. S. Huck, J. Genzer, M. Muller, C. Ober, M. Stamm, G. B. Sukhorukov, I. Szleifer, V. V. Tsukruk, M. Urban, F. Winnik, S. Zauscher, I. Luzinov, S. Minko, *Nat. Mater.* **2010**, *9*, 101–113; b) I. Tokarev, S. Minko, *Adv. Mater.* **2009**, *21*, 241–247; c) I. Tokarev, S. Minko, *Adv. Mater.* **2010**, *22*, 3446–3462; d) L.-Y. Chu, *Smart Membrane Materials and Systems*, Springer, Berlin-Heidelberg **2011**.
[4] a) S. Ladet, L. David, A. Domard, *Nature* **2008**, *452*, 76–79; b) J. Kopeček, J. Yang, *Angew. Chem. Int. Ed.* **2012**, *51*, 7396–7417.
[5] V. Kozlovskaya, E. Kharlampieva, I. Erel, S. A. Sukhishvili, *Soft Matter* **2009**, *5*, 4077.
[6] a) K. P. Loh, Q. Bao, P. K. Ang, J. Yang, *J. Mater. Chem.* **2010**, *20*, 2277; b) M. J. Allen, V. C. Tung, R. B. Kaner, *Chem. Rev.* **2009**, *110*, 132–145.
[7] a) H. W. Kim, H. W. Yoon, S.-M. Yoon, B. M. Yoo, B. K. Ahn, Y. H. Cho, H. J. Shin, H. Yang, U. Paik, S. Kwon, J.-Y. Choi, H. B. Park, *Science* **2013**, *342*, 91–95; b) R. K. Joshi, P. Carbone, F. C. Wang, V. G. Kravets, Y. Su, I. V. Grigorieva, H. A. Wu, A. K. Geim, R. R. Nair, *Science* **2014**, *343*, 752–754; c) B. Mi, *Science* **2014**, *343*, 740–742; d) H. Li, Z. Song, X. Zhang, Y. Huang, S. Li, Y. Mao, H. J. Ploehn, Y. Bao, M. Yu, *Science* **2013**, *342*, 95–98; e) R. R. Nair, H. A. Wu, P. N. Jayaram, I. V. Grigorieva, A. K. Geim, *Science* **2012**, *335*, 442–444; f) K. Raidongia, J. Huang, *J. Am. Chem. Soc.* **2012**, *134*, 16528–16531; g) D. A. Dikin, S. Stankovich, E. J. Zimney, R. D. Piner, G. H. B. Dommett, G. Evmenenko, S. T. Nguyen, R. S. Ruoff, *Nature* **2007**, *448*, 457–460; h) M. Hu, B. Mi, *Environ. Sci. Technol.* **2013**, *47*, 3715–3723.

[8] a) T. Kuilla, S. Bhadra, D. Yao, N. H. Kim, S. Bose, J. H. Lee, *Prog. Polym. Sci.* **2010**, *35*, 1350–1375; b) J. R. Potts, D. R. Dreyer, C. W. Bielawski, R. S. Ruoff, *Polymer* **2011**, *52*, 5–25; c) S. Stankovich, D. A. Dikin, G. H. B. Dommett, K. M. Kohlhaas, E. J. Zimney, E. A. Stach, R. D. Piner, S. T. Nguyen, R. S. Ruoff, *Nature* **2006**, *442*, 282–286; d) T. Ramanathan, A. A. Abdala, S. Stankovich, D. A. Dikin, M. Herrera-Alonso, R. D. Piner, D. H. Adamson, H. C. Schniepp, X. Chen, R. S. Ruoff, S. T. Nguyen, I. A. Aksay, R. K. Prud'homme, L. C. Brinson, *Nat. Nanotechnol.* **2008**, *3*, 327–331; e) C. Li, J. Adamcik, R. Mezzenga, *Nat. Nanotechnol.* **2012**, *7*, 421–427.

[9] a) H. G. Schild, *Prog. Polym. Sci.* **1992**, *17*, 163–249; b) P. W. Zhu, D. H. Napper, *J. Phys. Chem. B* **1997**, *101*, 3155–3160.

[10] X. Yang, L. Qiu, C. Cheng, Y. Wu, Z. F. Ma, D. Li, *Angew. Chem. Int. Ed.* **2011**, *50*, 7325–7328.

[11] a) K.-F. A. Gerald Gerlach, Springer, Berlin **2010**; b) K. Haraguchi, T. Takehisa, *Adv. Mater.* **2002**, *14*, 1120–1124; c) J.-Y. Sun, X. Zhao, W. R. K. Illeperuma, O. Chaudhuri, K. H. Oh, D. J. Mooney, J. J. Vlassak, Z. Suo, *Nature* **2012**, *489*, 133–136.

[12] a) J. K. Holt, H. G. Park, Y. Wang, M. Stadermann, A. B. Artyukhin, C. P. Grigoropoulos, A. Noy, O. Bakajin, *Science* **2006**, *312*, 1034–1037; b) M. A. Shannon, P. W. Bohn, M. Elimelech, J. G. Georgiadis, B. J. Marinas, A. M. Mayes, *Nature* **2008**, *452*, 301–310.

[13] F. Incropera, D. Dewitt, T. Bergman, A. Lavine, *Fundamentals of Heat and Mass Transfer*, 7th ed., Wiley, New Jersey **2007**.

[14] L. Qiu, X. Zhang, W. Yang, Y. Wang, G. P. Simon, D. Li, *Chem. Commun.* **2011**, *47*, 5810–5812.

[15] V. Georgakilas, M. Otyepka, A. B. Bourlinos, V. Chandra, N. Kim, K. C. Kemp, P. Hobza, R. Zboril, K. S. Kim, *Chem. Rev.* **2012**, *112*, 6156–6214.

[16] S.-B. Zhang, L.-Y. Chu, D. Xu, J. Zhang, X.-J. Ju, R. Xie, *Polym. Adv. Technol.* **2008**, *19*, 937–943.

[17] J. A. Jaber, J. B. Schlenoff, *Macromolecules* **2005**, *38*, 1300–1306.

[18] a) E. Krieg, B. Rybtchinski, *Chem. Eur. J.* **2011**, *17*, 9016–9026; b) B. Rybtchinski, *ACS Nano* **2011**, *5*, 6791–6818; c) E. Krieg, H. Weissman, E. Shirman, E. Shimoni, B. Rybtchinski, *Nat. Nanotechnol.* **2011**, *6*, 141–146; d) C. Schmuck, *Nat. Nanotechnol.* **2011**, *6*, 136–137.

[19] D. Li, M. B. Muller, S. Gilje, R. B. Kaner, G. G. Wallace, *Nat. Nanotechnol.* **2008**, *3*, 101–105.

[20] Y. Wang, X. Hou, C. Cheng, L. Qiu, X. Zhang, G. P. Simon, D. Li, *Aust. J. Chem.* **2014**, *67*, 168–172.